JOURNAL OF CATALYSIS 96, 189–201 (1985)

CoMo Sulfide Catalysts Studies by Metal Solid NMR: The Question of the Existence of the Chemical Synergy

MARC J. LEDOUX,* OLIVIER MICHAUX,* GIORGIO AGOSTINI,* AND PIERRE PANISSOD†

*Laboratoire de Catalyse et de Chimie des Surfaces, Université L. Pasteur, U.A. CNRS n° 423, and †Laboratoire de Magnétisme et de Structure Electronique des Solides, Université L. Pasteur, U.A. CNRS n° 306, Institut LeBel, 4 rue B. Pascal, 67070 Strasbourg Cedex, France

Received January 29, 1985; revised June 8, 1985

For the first time the ^{59}Co NMR has been used for the study of the cobalt sulfides in the Co-based HDS catalysts. Four different cobalt sites were observed on these catalysts, two of them corresponding to the regular octahedral and tetrahedral Co_9S_8 sites, the two other sites, one distorted tetrahedral and one octahedral, were only found in highly dispersed catalysts. A good correlation has been found between the HDS activity on Co/SiO_2 and Co/C catalysts and the amount of these new tetrahedral Co which are found very active. A parallel study of the HDS activity on mixed $CoMo/SiO_2$ has shown the classical so-called promoting effect of Co on Mo, but this effect can be simply described in terms of additivity of the Mo activity and of the new very active tetrahedral Co which are also observed to be dominant at the maximum of the volcano curve.

INTRODUCTION

Cobalt-promoted molybdenum catalysts supported on alumina, in their sulfided state are extensively used by the industry in hydrotreatment of petroleum feedstocks. An important controversy has arisen about the nature of the promotion on the hydrodesulfuration (HDS) when mixing Co to Mo. Mo sulfide (MoS_2) is generally considered as the least expensive catalyst (even if other sulfides have been found more reactive for the HDS (*1*)) and Co sulfide (Co_9S_8) as the promoter. Some years ago, Delmon (*2, 3*) proposed the "contact synergy model" where sulfur vacancies on MoS_2 at the boundary of the crystallites would be the site of the S-heterocompound adsorption, while on the other side of the boundary Co_9S_8, in close contact, would be the site of the H_2 adsorption–dissociation. Then the spill over of the hydrogen radicals would partly hydrogenate the adsorbed heterocompound, which will be split into hydrocarbon and H_2S. This process is known through Delmon's terminology as the "remote control process" (*4*). More recently, Topsøe *et al.* (*5*) have proposed a new structure of the sulfidic active phase, CoMoS, namely a decoration of the edges of small MoS_2 crystallites by Co atoms. They have been able to differentiate such a phase from the Co_9S_8 by the use of Mössbauer Emission Spectroscopy (MES) and to evaluate the amount of the different phases. They found a linear correlation between the amount of CoMoS phase and the HDS activity (*6*). Unfortunately, MES does not give much information about the structure of the different Co phases because of its poor resolution. The location of the Co atoms in the CoMoS phase is still hypothetical and Topsøe *et al.* (*7*) have proposed that these Co atoms are staying in interstitial position on the near edge of small MoS_2 crystallites; no more explicit information has been given by them on the nature and the structure of the active site except the fact that the stoichiometry seems to be one Co atom for one Mo atom in the pure CoMoS phase. In a different direction, Prins *et al.* (*8, 9*) have given evi-

0021-9517/85 $3.00

dence on the very high activity of CoMo catalysts supported on activated carbon; even activity of pure Co sulfide on this support is as high as the best CoMo supported on alumina. On the same support, Topsøe *et al.* (*7*) have found, with pure Co sulfide at low coverage, a doublet in the MES spectrum very similar to the one they attributed to the CoMoS phase in their other studies; this doublet evolves toward a broad single line corresponding to the Co_9S_8 line when the concentration of Co is increased.

Many physical techniques have been used in order to give information on the structure of the active phase of the CoMo sulfide system; however, most of them (XPS, TEM, IR, and UV reflectance, etc.) cannot reach the local order around the active metallic atoms, and EXAFS has until now not been able to solve the problem of the high chemical disorder surrounding the cobalt atoms (*10, 11*). Only MES has been able to show the presence of unexpected or exotic phases, but the proof of the presence of these new phases has sometimes been the result of mathematical deconvolution (*12, 13*).

For all these reasons, we have decided to investigate the cobalt sulfide structure in these materials by using the solid metal NMR technique.

EXPERIMENTAL

1. NMR

Our NMR measurements have been performed at 4.2 K for the sake of high sensitivity. A commercial Bruker CXP100 pulsed spectrometer equipped with a boxcar integrator has been used. The spectra were obtained using a spin-echo technique by scanning the magnetic field and digitally recording the spin-echo intensity yielded by the boxcar integrator versus the field intensity, H. The apparatus frequency was set at 15.2 MHz and the field was swept between 10 and 20 KOe, to cover the whole ^{59}Co NMR spectrum. In addition, the spectra were recorded for different time intervals (TI) between the spin-echo generating $\pi/2$-π pulse sequence. Such a technique provides an additional way to discriminate between different Co sites according to their eventually different longitudinal relaxation time T_1. Different Co sites are thus characterized by (i) their Knight shift (position of the spectrum) which is due to the supplementary field at the nucleus coming from the electronic, spin and orbital, magnetization; (ii) their quadrupolar frequency generated by the electric field gradient (if any) around the nucleus; (iii) their relaxation time T_1 which depends mainly upon the electronic density of states at the Fermi level in the metallic system under investigation. Because of the conduction electrons contributions to the NMR signal in metallic system, it is generally impossible to deduce, directly from the data, the coordination of the probed nucleus; one has to compare the data to the observations in model compounds which are used as finger prints.

Most of the structural information, then, is obtained from the measurement of the quadrupolar interaction which is closely related to the symmetry of the local environment. The local electronic structure which is given by the Knight shift and the relaxation time can be tentatively related to the catalytic activity and selectivity.

2. Preparation of the Catalysts and Experimental Conditions

—Four different supports have been used: high-purity nonacidic SiO_2 (Merck) pressed and sieved 0.2–0.5 mm after impregnation, high-purity nonacidic SiO_2 (Fluka) 0.5 mm, activated carbon Puriss (Fluka) 0.2–0.5 mm, and CK300 Ketjen γ-alumina, 0.2–0.5 mm. BET specific area: ~550 m^2/g for SiO_2, ~800 m^2/g for C, and ~220 m^2/g for Al_2O_3. After impregnation and calcination all the preparations were sieved 0.2–0.5 mm. The wetness impregnation method has been adopted on all the supports using aqueous solution of cobalt nitrate (Merck) or of ammonium paramo-

TABLE 1

Thiophene HDS Activities, 275°C, 1 atm H_2, 6 Torr Thiophene

Catalysts	$r \times 10^{-10}$ (mol/s · g cat.)	Conversion (%)	NTR (h^{-1})		
			per at. Mo	per at. Co	per at. Mo + Co
Co/SiO_2	In. 6475 ± 320	14.7	—	0.36	0.36 ± 0.03
38.3%	S.S. 6252 ± 300	15.1	—	0.35	0.35 ± 0.03
		(1.0–2.4)			(0.12 ± 0.01)
Co/SiO_2	In. 1881 ± 90	6.6	—	0.48	0.48 ± 0.03
8.4%	S.S. 1766 ± 90	6.1	—	0.45	0.45 ± 0.03
		(0.8–1.5)			(0.31 ± 0.03)
Co/SiO_2	In. 1008 ± 50	4.6	—	0.86	0.86 ± 0.04
2.5%	S.S. 838 ± 40	4.0	—	0.71	0.71 ± 0.03
		(0.3–0.8)			(0.37 ± 0.03)
$CoMo/SiO_2$	In. 7714 ± 380	17.4	3.62	3.57	1.80 ± 0.09
4.6/7.4%	S.S. 6806 ± 340	11.9	3.15	3.09	1.59 ± 0.08
		(0.6–1.2)			(0.53 ± 0.03)
$CoMo/SiO_2$	In. 12261 ± 600	27.3	5.11	9.66	3.34 ± 0.16
2.7/8.3%	S.S. 10146 ± 500	19.5	4.23	7.99	2.77 ± 0.13
		(0.6–1.3)			(1.11 ± 0.06)
Mo/SiO_2	In. 5308 ± 260	11.3	2.35	—	2.35 ± 0.12
7.8%	S.S. 4053 ± 200	8.9	1.79	—	1.79 ± 0.09
		(0.7–1.7)			(0.79 ± 0.04)
Mo/C	In. 6070 ± 300	16.3	5.35	—	5.35 ± 0.26
3.9%		(1.28)			(2.32 ± 0.12)
	S.S. 5036 ± 250	13.5	4.44	—	4.44 ± 0.22
Co/C	In. 10409 ± 520	21.8	—	2.64	2.64 ± 0.12
8.4%	S.S. 10534 ± 520	23.4	—	2.67	2.67 ± 0.12
Co/C	In. 9174 ± 460	22.0	—	6.85	6.85 ± 0.34
2.8%		(1.06)			(3.03 ± 0.15)
	S.S. 8166 ± 410	17.0	—	6.10	6.10 ± 0.31
		(1–4.5)			(3.08 ± 0.15)
$CoMo/Al_2O_3$ HR306	In. 14424 ± 700	33.7	6.25	13.15	4.24 ± 0.21
2.3/8.0%	S.S. 14993 ± 750	26.5	6.50	13.67	4.14 ± 0.22
Mo/Al_2O_3	In. 2923 ± 150	11.7	1.42	—	1.42 ± 0.21
7.1%	S.S. 2702 ± 140	10.1	1.31	—	1.31 ± 0.07

Note. In., initial; S.S., pseudo-steady state. Results at 220°C are shown in parentheses.

lybdate (Merck) (pH 5.5). When both molybdenum and cobalt were impregnated on a support, Mo was always impregnated first. Each impregnation was followed by two calcinations in air, the first for 12 h at 120°C and the second, for 2 h at 500°C. (Obviously, with C as support, the second calcination was canceled). In Table 1, first column, are reported the relative weight concentrations in metal and the nature of the support. A commercial $CoMo/Al_2O_3$ HR306 PROCATALYSE was used as standard for activity. Elemental analysis for metal was performed by atomic absorption (Service Central d'Analyse du CNRS).

—These preparations were all presulfided in the same condition. The required amount of catalyst (~300 mg for NMR anal-

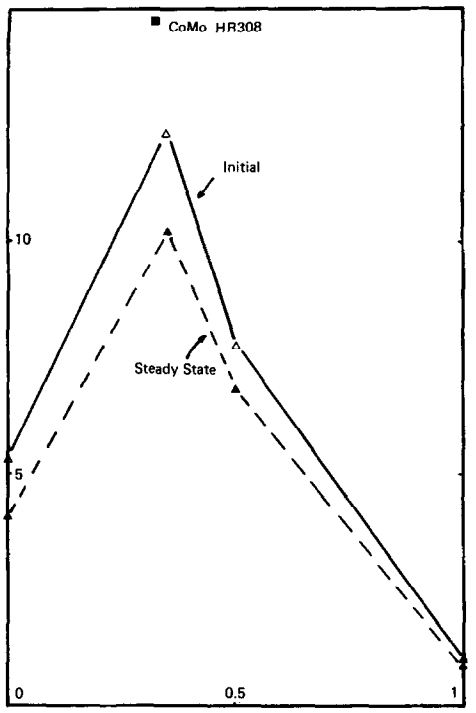

FIG. 1. Thiophene HDS specific activity (mol/s · g(cat.)) versus Co/Co + Mo on SiO_2, 290°C, 1 atm H_2, 6 Torr thiophene.

ysis and ~50 mg for HDS activity determination) was placed in the reactor, flushed at room temperature with pure H_2 for 15 min, then a mixture H_2S/H_2 2% was switched on and the temperature raised to 450°C (13°C/min), then left for 2.5 h at this temperature under a flow of 150 cm^3/min at normal pressure. At this stage, the reactor was either cooled down to room temperature in 5 min and the catalyst transferred under argon in the Teflon sample holder (NMR analysis before reaction), or was cooled to 290°C. The flow was switched to pure H_2 (~100 cm^3/min for 5 min), then thiophene was introduced under constant partial pressure of 6 Torr. A first measure was made after 4 min (initial activity) where the reaction products were sampled and analyzed by chromatography; a second measure after 1 h and a third after 2 h were also made (pseudo-steady state). In all cases this pseudo-steady state (15% lower than the initial activity) was reached after 2 h under flow (no change in activity after 48 h on run); for Co/C 8.4% and $CoMo/Al_2O_3$ HR306 the initial activity was not really affected. However, for Mo/C 4%, the pseudo-steady state was only reached after 24 h. The conversion was kept as low as possible, below 20% for most of the cases, the rate of the reaction being obtained from the classical fixed-bed differential reactor integrated equation

$$r = (1 - \alpha) \cdot \ln\left(\frac{1}{1 - \alpha}\right) \cdot \frac{F}{w},$$

where α is the conversion, F the flow of thiophene, and w the catalyst weight. The test apparatus was described elsewhere (*14, 15*). In order to work in real differential condition, the reaction has also been perform at 227°C under 19 Torr of thiophene, at very low conversion. The rate has been obtained by varying the space velocity (four points), the conversion has always been found proportional to the inverse of the space velocity.

RESULTS

1. Catalysis (HDS)

In Table 1 are reported the activities of the different catalysts. The second column shows the specific activity in moles of thiophene transformed per second and per gram of catalyst and the third column shows the conversion. The three following columns show the different nominal turnover rate (NTR) assuming that both Co and Mo atoms are all accessible and assuming also that a site is monoatomic in Mo or Co. In addition, in the sixth column, one assumes that a Co site has the same activity than a Mo site.

In Fig. 1, the classical promotion effect (*16*) with a profile of a volcano curve is observed for the catalysts containing ~8% of Mo when varying the Co concentration on SiO_2. The best catalyst of this series presents an initial activity almost equal to the commercial $CoMo/Al_2O_3$ HR306, al-

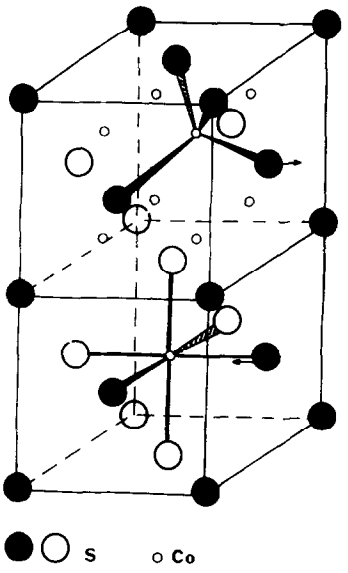

FIG. 2. Unit cell Co_9S_8.

though this commercial catalyst does not lose activity with time even after 3 days in our reaction conditions.

In Table 1, one can see that the carbon supported catalysts (Mo or Co) exhibit a very high initial activity and confirm the results found by Prins *et al.* (*8*).

2. NMR

In order to obtain a fingerprint of the NMR signal arising from ^{59}Co in the Co_9S_8 compound, we have first examined the case of a highly loaded Co/SiO_2 38% sulfided catalyst. Alumina-supported catalysts could not be studied under these conditions because at the frequency which we used, aluminum NMR impairs the Co sulfided ones.

Co_9S_8 contains in its unit cell (Fig. 2), eight Co atoms in tetrahedral configuration (TC) inside a fcc sulfur structure and one Co atom in octahedral configuration (OC) inside another fcc sulfur structure. In the first sulfur cube, the atoms at the face center are slightly out of the plane while in the second cube, the sulfur atoms are slightly inside the cube. Each of these cubes is surrounded by six cubes of the other family in a three-dimensional checkered structure.

The NMR spectrum observed in this compound is shown in Fig. 3. It consists of nine peaks: eight peaks split by the quadrupolar interaction for the Co sites in TC and one peak for the Co site in OC which has a cubic point symmetry. The quadrupole interaction obtained by simulation (Figs. 3 and 4) for TC is found to be $e^2 \cdot q \cdot Q/h = 26.3 \pm 0.2$ MHz. The Knight shift is $K = 0.71 \pm 0.05\%$ with respect to $\gamma_{Co}/2\pi = 1.0103$ kHz/Oe for both sites (OC and TC) but the longitudinal relaxation time T_1 is found drastically different on the two sites; about 11 ms for TC and a long 350 ms for OC reflects the very different electronic surrounding of Co in the two sites (Fig. 5).

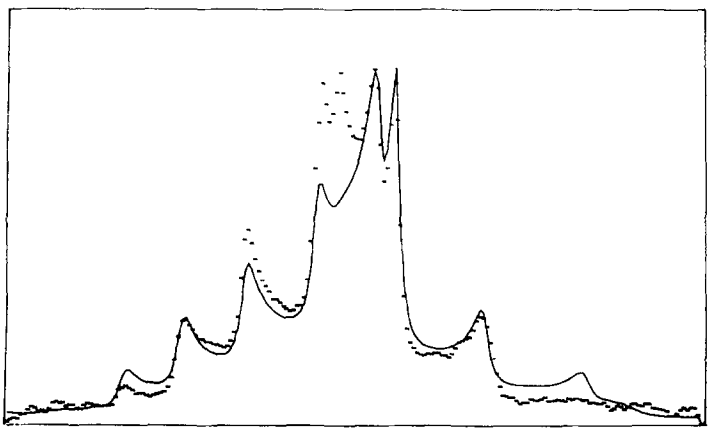

FIG. 3. Full spectrum. Co/SiO_2 38%. Full line: simulation with 8 tetrahedral sites. Dotted line: spectrum containing also the octahedral site.

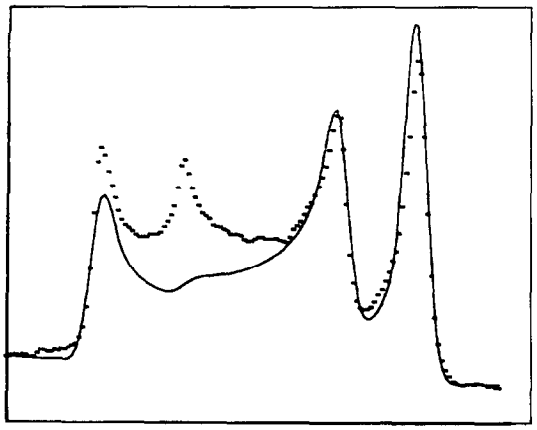

FIG. 4. Central line (as for Fig. 3).

This difference can result from the proximity of the three Co neighbors of the TC sites while there is no metallic neighbor inside the sulfur cube on the OC sites and from a difference of the symmetry of the highest occupied *d* orbital (see Discussion).

Figure 5 shows the central part of the Co spectrum for two different time intervals (*TI*) between the measurements pulse sequence: for the slow repetition rate (*TI* = 400 ms) the spectrum exhibits the strong singlet of the OC resonance while for a much shorter *TI* (10 ms), this resonance is totally saturated and the OC peak vanishes. For *TI* $\geqq$ 1 s, the OC signal has reached its full intensity and the area ratio of the spectra corresponding to the two Co sites, 1/9 for OC and 8/9 for TC is established (Fig. 6).

The simulation, the correct values for the Co atoms ratio and the absence of any other signal including the Co oxides confirm that on the Co/SiO_2 38% catalyst, only Co_9S_8 is present after the used presulfiding conditions. Unless otherwise specified, the short *TI* (10 ms) condition has been used for the measurements, so that the signal of OC in Co_9S_8 is nearly totally absent from the spectra.

In Fig. 7, the same result concerning the relaxation time is observed for the catalyst Co/SiO_2 8.4%. In Fig. 8, the NMR spectra (central band) of the same catalyst recorded before and after reaction show that the Co

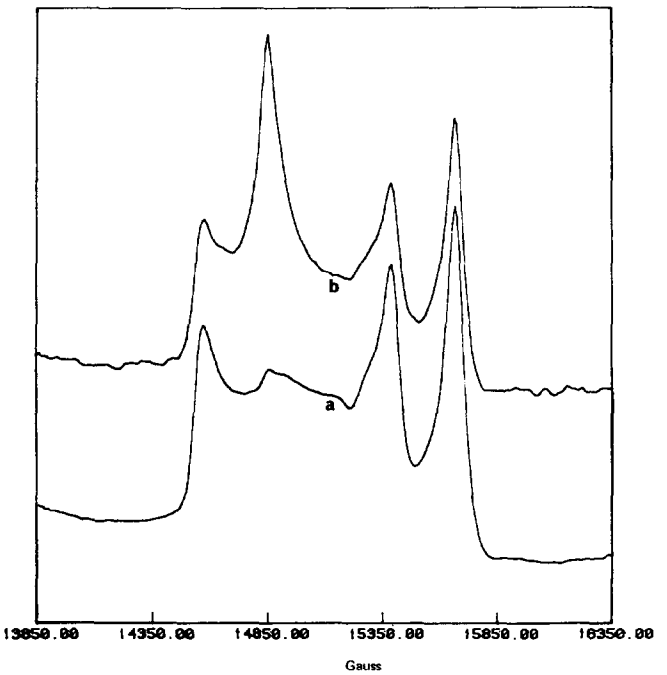

FIG. 5. Central line. Co/SiO_2 38%. (a) *TI* = 10 ms, (b) *TI* = 400 ms.

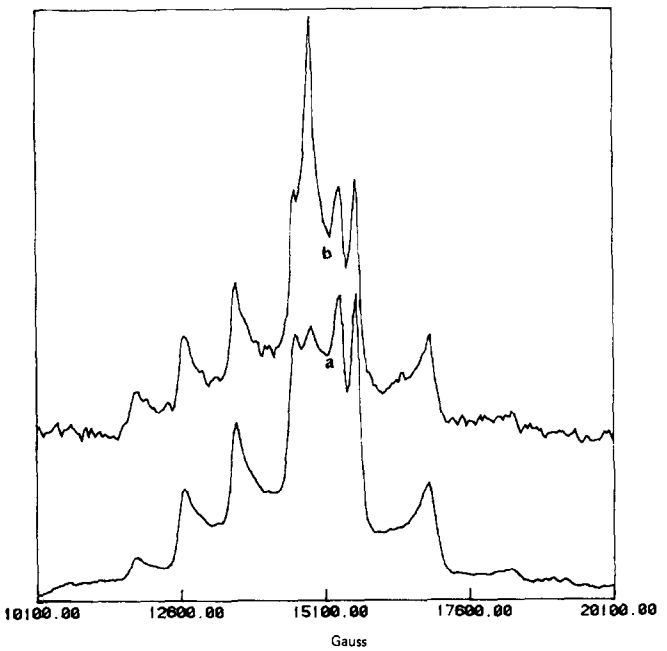

FIG. 6. Full spectra. Co/SiO_2 38%. (a) TI = 10 ms, (b) TI = 400 ms.

structure and configuration are not modified by the reaction. The same fact has been observed for the other catalysts (checked on $CoMo/SiO_2$, 2.7/8.3% and 4.6/7.4%). Thus, the deactivation of the catalyst during the reaction is probably due to the sintering of the Mo sulfide (see Discussion).

The effect of dispersion obtained by the

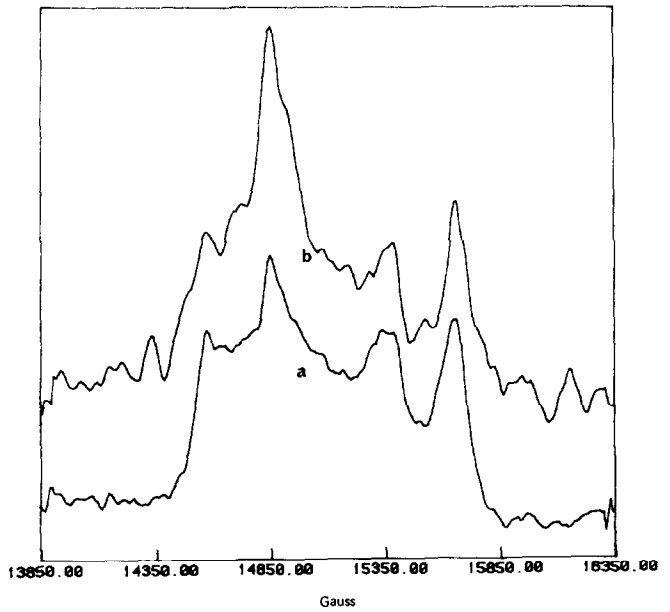

FIG. 7. Central line. Co/SiO_2 8%. (a) TI = 10 ms, (b) TI = 400 ms.

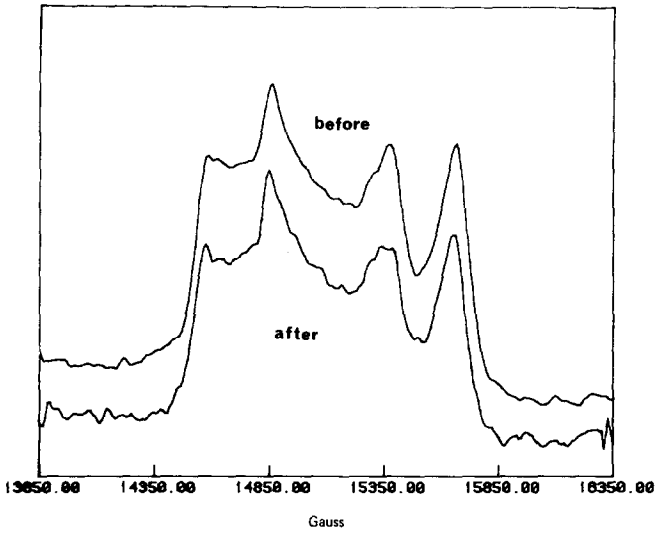

FIG. 8. Central line. *TI* = 10 ms. Co/SiO_2 8%. Before and after reaction.

dilution of the Co on the silica (Co/SiO_2, 38, 8, and 2.5%) is important on the structure of the sulfided phase. In Figs. 9a, b, and c, the evolution of the central band shows a significant broadening of the TC signal and the appearance of a single line at the position of OC sites but with a short relaxation time. The sites corresponding to this new line are probably octahedrally coordinated as OC Co's in Co_9S_8 but their relaxation time indicates that their local electronic environment is comparable to that of TC Co's (see Discussion).

It is interesting to note that in Co_9S_8 the sulfur atoms form a nearly fcc lattice which differs from the hexagonal lattice of S in CoS (cobalt monosulfide) only by a different piling up of the (111) fcc planes. In CoS Co atoms are in a nearly octahedral sulfur coordination and they have two Co neighbors at 2.56 Å while TC Co's in Co_9S_8 have three neighbors at 2.50 Å and OC Co's none. Thus it is suggested that the highly dispersed Co sulfided catalysts have a microcrystalline Co_9S_8 structure, where a great number of Co atoms located on defects, grain boundaries, and surface atoms would be in a octahedral configuration with still a fair amount of Co neighbors (locally

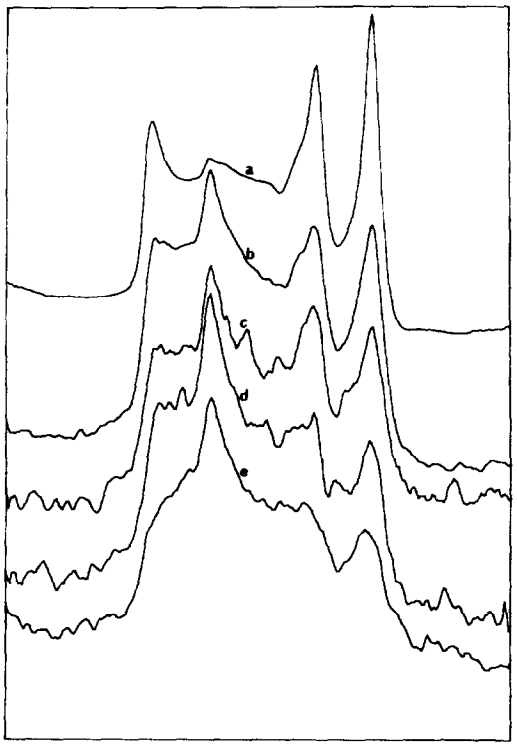

FIG. 9. Central line. *TI* = 10 ms. (a) Co/SiO_2 38%, (b) Co/SiO_2 8%, (c) Co/SiO_2 2.5%, (d) $CoMo/SiO_2$ 4.6/7.4%, (e) $CoMo/SiO_2$ 2.7/8.3%.

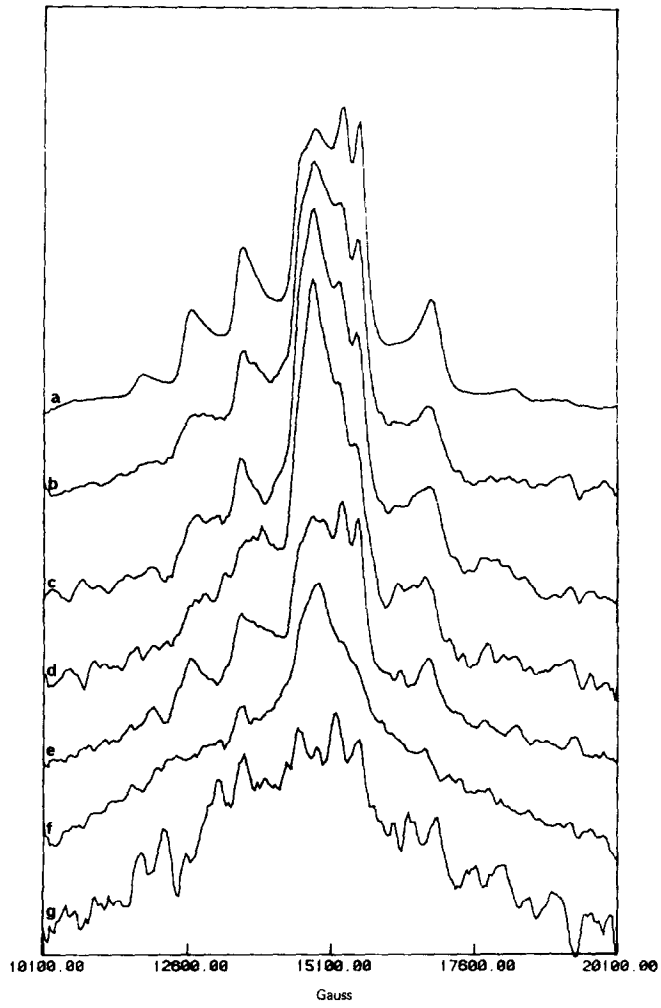

FIG. 10. Full spectra. TI = 10 ms. (a) Co/$SiO_2$38%, (b) Co/SiO_2 8%, (c) Co/SiO_2 2.5%, (d) CoMo/SiO_2 4.6/7.4%, (e) Co/C 8.4%, (f) CoMo/SiO_2 2.7/8.3%, (g) Co/C 2.8%.

CoS like). A possible explanation would be that because of the dispersion, not all the cubes containing the eight TC Co are surrounded by the regular cubes containing the OC Co atoms; the TC Co, during the sulfidation, would then capture sulfur atoms outside the regular unit cell in order to replace the vacant cubes (for instance, at grain boundaries or on the surface).

The evolution due to the dispersion (TC broadening) is regularly proceeding in the same direction on the two catalysts containing Mo (Figs. 9d, e) which indicates that the molybdenum sulfide acts as a superdispersant for the Co sulfide. As the activity of the catalyst reported per Co atom is increasing with the occurrence of the octahedral Co atoms with short relaxation time one can be tempted to consider these atoms as the site for the HDS reaction. However, on carbon supported Co catalysts (Figs. 10e and g), these atoms with short relaxation time are totally absent and yet the activity per Co atom of this catalyst is very high and comparable to or even higher than the activity of CoMo/SiO_2.

The correlation between activity and a particular structure can be found by the

study of the total spectra of the different catalysts (Fig. 10). Indeed when the dispersion is increasing from Co/SiO_2 38% to Co/C 2.8%, the appearance of a broad underline spectrum reminiscent of TC in Co_9S_8, amorphous or microcrystalline, under the structure of the well-cristallized Co_9S_8 spectrum, can be quantitatively related to the HDS activity (see Discussion).

Thus it is in our opinion that when highly dispersed, Co sulfide is a highly active HDS catalyst with an activity comparable to that of highly dispersed MoS_2. It is then necessary to reconsider the so-called synergetic behaviour of the CoMo sulfide mixture in terms of a possible addition of the activities of both Mo and Co sites.

DISCUSSION

Pecoraro and Chianelli (*1*) found a factor of about 5 between the dibenzothiophene HDS activity of Mo and Co bulk sulfide, expressed in converted mole per second and per mole of metal sulfide; we found the same factor between Mo/SiO_2 7.8% and Co/SiO_2 38%. In order to explain these differences in activity when changing the nature of the metal, Harris and Chianelli (*18*) have evaluated the electronic population in the molecular orbital (MO) of the octahedral clusters MS_6^{n-} by SCF-Xα calculation. After many attempts, they found that the best correlation between activity and electronic factor is given by a parameter A_2 which is the product of the number of d electrons in the HOMO (highest occupied molecular orbital) of the cluster by a factor B which measures together (i) the number of bonding electrons in the $2e_g(\sigma)$ and in the $1t_{2g}(\pi)$ MO (ii) the metal d orbital contributions to these MOs (covalency). All the calculations supposed an octahedral cluster where the metal d orbitals in low spin are split in two sets, the t_{2g} (6 electrons) at lower energy than the e_g (4 electrons). (The largest discrepancy between the calculated parameter and the measured activity was found for Co and Ni while for Mo the agreement was remarkable.) If as we have seen, the active Co sites have a tetrahedral configuration, and if the hypothesis of low spin is maintained, the e_g levels should lie below the t_{2g} levels and the value of A_2 will be modified. The number of electron in the HOMO would be now about 3 (if most of the metal character is attributed to the highest MOs) in the $2t_{2g}$ (1 in $3e_g$ in the octahedral configuration). This value of 3 in the right symmetry ($2t_{2g}$) is precisely the electronic configuration of Mo calculated by Harris and Chianelli. One must thus expect a comparable HDS activity for Co tetrahedral and for Mo octahedral. The discrepancy observed by these authors for Co could be due to the fact that the measured HDS activity reflected a partly tetrahedral behavior while the calculated factor took in account only an octahedral configuration. A confirmation of our hypothesis is given by the calculation of the Fermi level (HOMO) density of states from the NMR measurements which is at least three times higher for the tetrahedral Co sites than for the isolated octahedral Co sites in Co_9S_8. This difference between the densities of states is reflected mostly by the strong difference between the T_1's of Co in the two configurations (a similar analysis of K and T_1 can be found for copper dichalcogenides in Ref.(*17*)).

Another very interesting point can be explained through the Harris and Chianelli theory. As mentioned above, the NMR study suggests that when the dispersion of Co_9S_8 is very high, some of the Co atoms in tetrahedral sites become octahedral by the capture of extra sulfur atoms. In this intermediate situation between tetrahedral and octahedral, the metal d orbital could be restricted in a high-spin configuration without the splitting of the t_{2g} and e_g levels, the density of states at the Fermi level would be high even in an octahedral configuration which is consistent with the short relaxation time. In the CoMo-sulfided catalysts such octahedral atoms could be localized at the boundaries between Co sulfide and Mo sulfide and act as a glue to stabilize the highly dispersed active tetrahedral Co. This

description of the contact between Co sulfide and Mo sulfide corresponds exactly to a model that Harris has developed in a recent communication (*19*). She found an extrastabilization for Co and Ni because the energy of the *d* orbitals of these two metals (poorly split, almost high spin) lies between the two sets of the 4*d* Mo orbitals. In the case of ($S_3CoS_3MoS_3$) the result of the combination is a transfert of one electron from Co toward Mo (3 electrons for Ni). Such a transfert has already been predicted by XPS measurements (*20*) or by chemical deduction (*15*).

A model of the active surface emerges from these electronic considerations, where the Mo sulfide is active but not necessarily improved or dispersed by the presence of Co sulfide and where the nature of the Co sulfide is deeply modified by the presence of Mo. The large amount of active tetrahedral Co is stabilized by an interphase of octahedral Co, sharing three sulfur atoms with MoS_2 edges.

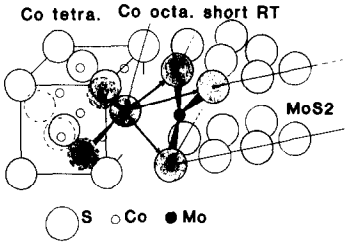

On carbon, because of the very small size of the pores, only sulfur cubes containing tetrahedral Co are formed at low concentration of Co. One can attempt to correlate the amount of the tetrahedral active Co determined by NMR to the activity measured on the different catalysts.

First, three hypothesis must be settled:

(A1) Each site, Mo or Co, is chemically independent of its neighbors concerning its HDS activity; the total activity is only the addition of the Co and the Mo activity.

(A2) Mo/C 3.9% exhibits the highest catalytic accessibility (which we define as the percentage of active Mo atoms/total number of Mo atoms) for Mo at initial activity, 100%, with a NTR of 5.35 h^{-1}.

TABLE 2

Calculation of the Catalytic Accessibility for the One-Metal Catalysts

Mo/SiO_2 7.8%	NTR = 1.79	x_{Mo} = 33% (34)
Co/SiO_2 38%	NTR = 0.35	x_{Co} = 5% (4)
Co/SiO_2 8%	NTR = 0.45	x_{Co} = 7% (10)
Co/SiO_2 2.5%	NTR = 0.71	x_{Co} = 10% (12)
Co/C 8.4%	NTR = 2.67	x_{Co} = 39%

Note. Values for 220°C are shown in parentheses.

(A3) Co/C 2.8% exhibits the highest catalytic accessibility of Co at initial activity, 100%, with a NTR of 6.85 h^{-1}. (If the catalytic accessibility in these two examples are less than 100%, then all the following results will be displaced similarly, but still valid.)

From these hypothesis, one can deduce the catalytic accessibilities x reported in the Table 2.

A general equation for the CoMo catalysts can be written NTR/Mo + $Co_{(measured)}$ = (% atom Mo) · x_{Mo} · (5.35) + (% atom Co) · x_{Co} · (6.85). As there is no experimental access to the catalytic accessibility of Mo on these catalysts (O_2, CO, NO chemisorption still controversial for mixed catalysts), one is reduced to examining three hypothesis:

(H_1) Mo is not dispersed by Co, only Co is dispersed by Mo, thus x_{Mo} = 33%.

(H_2) Mo is identically dispersed by Co as Co is dispersed by Mo; thus $x_{Co} = x_{Mo}$.

(H_3) For each Mo active corresponds one Co active; thus % atom Mo · x_{Mo} = % atom Co · x_{Co}.

One can now obtain the calculated values of x_{Mo} and x_{Co} for the two CoMo catalysts and compare the x_{Co} for all the catalysts to the percentage of Co contained in the broad underline spectrum attributed to amorphous or microcrystalline tetrahedral Co sulfide (Table 3).

A good agreement is found if one considers either Hypothesis 1 or 3. The high values of the broad line in Co/SiO_2 8%, 2.5% and CoMo 4.6/7.4% compared to the values of x_{Co} in H_1 or H_3 are probably due to

TABLE 3

Correlation between HDS Activity and NMR Measurements

Catalyst	Catalysis							NMR		
	NTR/Co + Mo (h^{-1}, S.S.)	x_{Mo} in %			x_{Co} in %			% of act. tetrahed. Co	% of Co_9S_8	% of rapid octah. Co
		H_1	H_2	H_3	H_1	H_2	H_3			
Co 38%	0.35	—	—	—	5	5	5 (4)	5[a]	95	2
Co 8%	0.45	—	—	—	7	7	7 (10)	19 ± 5	72	9
Co. 2.5%	0.71	—	—	—	10	10	10 (15)	19 ± 9	67	14
CoMo 4.6/7.4%	1.59	33 (34)	26	26 (20)	21	26	26 (20)	37 ± 5	49	14
CoMo 2.7/8.3%	2.77	33 (34)	47	35 (32)	68	47	65 (59)	75 ± 8	18	7
Co/C 8.4%	2.67	—	—	—	39	39	39	31 ± 7	69	0
Co/C 2.8%	6.85[b]	—	—	—	100%[c]			>90	<10	0

Note. Values for 220°C are shown in parentheses.

[a] Assumed.

[b] Initial NTR.

[c] By convention.

the fact that for these three catalysts the dispersion of the Co sulfide is relatively bad, and some distorded tetrahedral Co are located on grain boundaries or defects inside the bulk and are not accessible for catalysis. On the contrary, for the other catalysts where the dispersion is high (carbon supported or maximum interaction with Mo) the correlation is better.

Finally, the deactivation observed between initial and pseudo-steady state activity cannot be attributed to a sintering or a recristallization of the Co phases because the NMR spectra of ^{59}Co taken before and after reaction are identical. A possible deactivation due to the deposition of coke residue, must also be rejected after such a short time in reaction, because low temperature (290°C) and small molecule (thiophene) associated with nonacidic support are not the conditions leading to a significant coking. However, the possibility of coking after a very long time is not excluded; this is why we used "pseudo-steady state" through out the text. Thus, the last possibility is a sintering of the Mo sulfide. The fact that CoMo HR306, where the dispersion of Mo has been carefully optimized, does not lose activity, and the fact that Mo/C, where the usual strong interaction between Mo and the support does not occur, took a long time to reach the steady state, are both confirming the role of the Mo sintering. In addition, we have strong evidence that partial desulfuration of pure Mo catalysts is important in our condition (*21*).

CONCLUSION

This study has shown, in Co/SiO_2 and Co/C catalysts, the existence besides the regular Co_9S_8, of a highly dispersed Co sulfide phase which consists of Co inside very distorted sulfur tetrahedra reminiscent of the Co_9S_8 tetrahedral Co sites. This new phase, which looks like an amorphous structure, has been found responsible for the high activity of Co/C catalysts. Such high

activity can be explained in the framework of the Harris and Chianelli theory since as indicated by the NMR data, the electronic state is similar in terms of population and symmetry to the octahedral Mo electronic structure. This phase, which is probably the one observed by Topsøe *et al.*, is found to be dominant in CoMo catalysts at the maximum HDS activity. Consequently, the so-called synergetic effect of Co on Mo can in fact be simply interpreted in terms of additivity of the MoS_2 and the new Co "phase" activities as shown by our quantitative analysis. In addition, we have also observed other new Co sites octahedrally coordinated, different from the regular Co_9S_8 octahedral sites, the amount of which cannot be related to the HDS activity but which might be necessary to stabilize the high dispersion of the new tetrahedral Co network at the interface with MoS_2 rafts. In addition, the existence of these octahedral Co's can suggest in the new quasiamorphous Co sulfide phase, a competition between the formation of active tetrahedral Co's and inactive octahedral Co's.

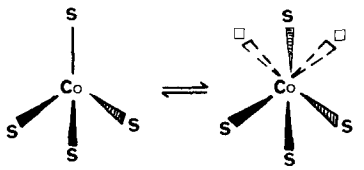

The stability of the tetrahedral configuration together with the favorable orbital symmetry (t_{2g}) balanced by the geometrical possibility to form an octahedral environment provide a good illustration of the Sabatier principle.

ACKNOWLEDGMENT

M.J.L. wishes to acknowledge the partial support of this research by the DRRT (Action Régionale n° 83.J.0365) and the ANVAR-Alsace (n°A8302008 A003-0).

REFERENCES

1. Pecoraro, T. A., and Chianelli, R. R., *J. Catal.* **67,** 430 (1981).
2. Hagenbach, G., Courty, P., and Delmon, B., *J. Catal.* **23,** 295 (1971).
3. Delmon, B., *in* "Proceedings, 3rd International Conference on the Chemistry and the Uses of Molybdenum," Ann Arbor, Michigan" (H. F. Barry and P. C. H. Mitchell, Eds.), p. 73. 1980.
4. Pirotte, D., Zabala, J. M., Grange, P., and Delmon, B., *Bull. Soc. Chim. Belg.* **90,** 1239 (1981).
5. Topsøe, H., Clausen, B. S., Candia, R., Wivel, C., and Morup, S., *J. Catal.* **68,** 433 (1981).
6. Candia, R., Clausen, B. S., and Topsøe, H., *J. Catal.* **77,** 564 (1982).
7. Topsøe, H., Candia, R., Topsøe, N. Y., and Clausen, B. S., *Bull. Soc. Chim. Belg.* **93,** 783 (1984).
8. Duchet, J. C., Van Oers, E. M., De Beer, V. H. J., and Prins, R., *J. Catal.* **80,** 386 (1983).
9. Vissers, J. P. R., Groot, C. K., Van Oers, E. M., De Beer, V. H. J., and Prins, R., *Bull. Soc. Chim. Belg.* **93,** 813 (1984).
10. Candia, R., Clausen, B. S., Bartholdy, J., Topsøe, N. Y., Lengeler, B., and Topsøe, H., *in* "Proceedings, 8th International Congress on Catalysis, Verlag Chemie, Weinheim, Berlin," p. II.375. 1984.
11. Boudart, M., Arrieta, J. S., and Dalla Betta, R., *J. Amer. Chem. Soc.* **105,** 6501 (1983).
12. Göbölös, S., Wu, Q., Ladriere, J., Delannay, F., and Delmon, B., *Bull. Soc. Chim. Belg.* **93,** 687 (1984).
13. Clausen, B. S., Mørup, S., Topsøe, H., and Candia, R., *J. Phys. Colloq.* **37,** C6-249 (1976).
14. Ledoux, M. J., Esteban Puges, P., and Maire, G., *J. Catal.* **76,** 285 (1982).
15. Ledoux, M. J., Agostini, G., Benazouz, R., and Michaux, O., *Bull. Soc. Chim. Belg.* **93,** 635 (1984).
16. Yermakov, Y. I., Startsev, A. N., and Burmistrov, V. A., *Appl. Catal.* **11,** 1 (1984).
17. Krill, G., Panissod, P., Lapierre, M. F., Gauthier, F., Robert, C., and Nassr Eddine, M., *J. Phys. C Suppl.* **9,** 1521 (1976).
18. Harris, S., and Chianelli, R. R., *J. Catal.* **86,** 400 (1984).
19. Harris, S., Abstract, 1984 Fall Meeting MRS Boston, p. 173 (1984).
20. Alstrup, I., Chorkendorff, I., Candia, R., Clausen, B. S., and Topsøe, H., *J. Catal.* **77,** 397 (1982).
21. Ledoux, M. J., Michaux, O., Agostini, G., to be published.